

Iron(II) Complexes Bearing Tridentate PNP Pincer-Type Ligands as Catalysts for the Selective Formation of 3-Hydroxyacrylates from Aromatic Aldehydes and Ethyldiazoacetate

David Benito-Garagorri,[†] Julia Wiedermann,[†] Martin Pollak,[†] Kurt Mereiter,[‡] and Karl Kirchner^{*,†}

Institute of Applied Synthetic Chemistry and Institute of Chemical Technologies and Analytics, Vienna University of Technology, Getreidemarkt 9, A-1060 Vienna, Austria

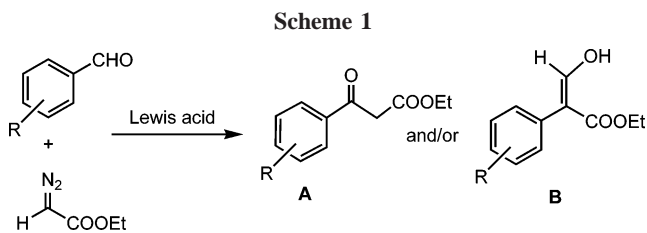
Received September 4, 2006

Several new iron(II) complexes of the types $[\text{Fe}(\text{PNP})(\text{CO})(\text{CH}_3\text{CN})_2]^{2+}$, $[\text{Fe}(\text{PNP})(\text{CO})_2\text{Br}]^+$, and $\text{Fe}(\text{PNP})\text{Cl}_2$ containing tridentate PNP pincer-type ligands have been prepared and characterized. Some of them turned out to be efficient catalysts for the coupling of aromatic aldehydes with ethyldiazoacetate (EDA) to give 3-hydroxyacrylates. These reactions are highly chemoselective, proceed under mild conditions, exhibit good scope, and circumvent the need of slow addition of EDA at low temperature.

Introduction

Aromatic aldehydes are known to react with ethyldiazoacetate (EDA) in the presence of Lewis acids such as BF_3 , ZnCl_2 , AlCl_3 , GeCl_2 , and SnCl_4 to give mainly 3-oxo-3-arylpropanoic acid ethyl esters (β -ketoesters) (**A**) in high yields (Scheme 1).^{1–3} Recently, Hossain and co-workers have found that the cyclopentadienyl dicarbonyl Lewis acid $[\text{FeCp}(\text{CO})_2(\text{THF})]\text{BF}_4$ is an active catalyst for the coupling of aromatic aldehydes with EDA to afford 3-hydroxy-2-arylacrylic acid ethyl esters (3-hydroxyacrylates) (**B**) as the main product (Scheme 1).⁴ Similar results were obtained by the same authors with the Brønsted acid $\text{HBF}_4 \cdot \text{Et}_2\text{O}$ as catalyst.⁵ This methodology was applied to the synthesis of a naproxen precursor, a highly valued anti-inflammatory drug.^{4b} Moreover, the coupling of salicylaldehydes with EDA, also reported by Hossain and co-workers, gives access to the preparation of benzofurans, which can be used as building blocks in the synthesis of several biologically active compounds.⁶

However, in these cases slow addition of EDA over a period of 6–7 h at low temperature is required, and in addition substantial amounts of β -keto esters are typically formed. Similar results were also described recently by Kanemasa et al. by utilizing ZnCl_2 in the presence of chlorotrimethylsilane as catalyst.⁷ Herein we describe a new class of iron catalysts⁸ that



are capable of mediating the direct coupling of aromatic aldehydes with EDA to give chemoselectively 3-hydroxyacrylates in high isolated yields. The iron compounds tested as catalysts bear PNP pincer ligands based on 2,6-diaminopyridine and 2,6-diamino-4-phenyl-1,3,5-triazine as shown in Chart 1. The ability to coordinate to metal centers very strongly makes pincer ligands excellent candidates for the design of well-defined catalysts since electronic, steric, and even stereochemical properties can be varied easily in modular fashion.⁹

Results and Discussion

Synthesis of Fe(PNP) Complexes. Treatment of $[\text{Fe}(\text{PNP}-\text{Ph})(\text{CH}_3\text{CN})_3]^{2+}$ (**1a**) and $[\text{Fe}(\text{PNP}-i\text{Pr})(\text{CH}_3\text{CN})_3]^{2+}$ (**1b**) with CO affords the monocarbonyl complexes *cis*- $[\text{Fe}(\text{PNP}-\text{Ph})(\text{CO})(\text{CH}_3\text{CN})_2]^{2+}$ (**2a**) and *cis*- $[\text{Fe}(\text{PNP}-i\text{Pr})(\text{CO})(\text{CH}_3\text{CN})_2]^{2+}$ (**2b**) in 88 and 93% isolated yields, respectively (Scheme 2). There was no evidence for the formation of dicarbonyl complexes $[\text{Fe}(\text{PNP})(\text{CO})_2(\text{CH}_3\text{CN})]^{2+}$. On the other hand, with $[\text{Fe}(\text{PNP}-\text{BIPOL})(\text{CH}_3\text{CN})_3]^{2+}$ (**1c**), where the PNP ligand contains the stronger π -accepting BIPOL units, no reaction took place.

Characterization of complexes **2a** and **2b** was accomplished by elemental analysis and ^1H , $^{13}\text{C}\{^1\text{H}\}$, and $^{31}\text{P}\{^1\text{H}\}$ NMR and IR spectroscopy. In addition, the solid-state structure of *cis*- $[\text{Fe}(\text{PNP}-i\text{Pr})(\text{CO})(\text{CH}_3\text{CN})_2](\text{BF}_4)_2$ (**2b**) was determined by single-crystal X-ray diffraction. These complexes exhibit a

* Corresponding author. E-mail: kkirch@mail.zserv.utwien.ac.at.

[†] Institute of Applied Synthetic Chemistry.

[‡] Institute of Chemical Technologies and Analytics.

(1) (a) Holmquist, C. R.; Roskamp, E. J. *J. Org. Chem.* **1989**, *54*, 3258. (b) Holmquist, C. R.; Roskamp, E. J. *Tetrahedron Lett.* **1992**, *33*, 1131.

(2) (a) Padwa, A.; Hornbuckle, S. F.; Zhang, Z.; Zhi, L. *J. Org. Chem.* **1990**, *55*, 5297. (b) Sudrik, S. G.; Balaji, B. S.; Singh, A. P.; Mitra, R. B.; Sonawane, H. R. *Synlett* **1996**, 369.

(3) Nomura, K.; Iida, T.; Hori, K.; Yoshii, E. *J. Org. Chem.* **1994**, *59*, 488.

(4) (a) Mahmood, S. J.; Hossain, M. M. *J. Org. Chem.* **1998**, *63*, 3333. (b) Mahmood, S. J.; Brennan, C.; Hossain, M. M. *Synthesis* **2002**, 1807.

(5) Dudley, M. E.; Morshed, Md. Monzur; Brennan, C. L.; Islam, M. S.; Ahmad, M. S.; Atuu, M.-R.; Branstetter, B.; Hossain, M. M. *J. Org. Chem.* **2004**, *69*, 7599.

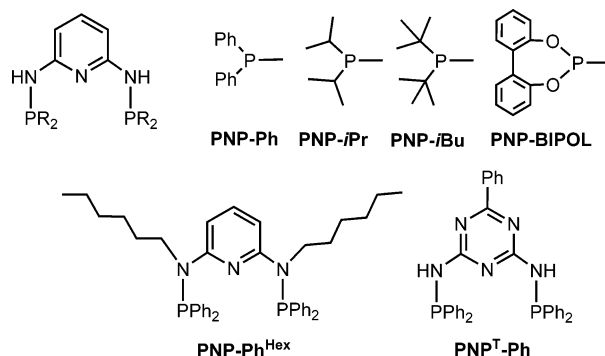
(6) Dudley, M. E.; Morshed, M. M.; Hossain, M. M. *Synthesis* **2006**, *10*, 1711.

(7) Kanemasa, S.; Kanai, T.; Araki, T.; Wada, E. *Tetrahedron Lett.* **1999**, *40*, 5055.

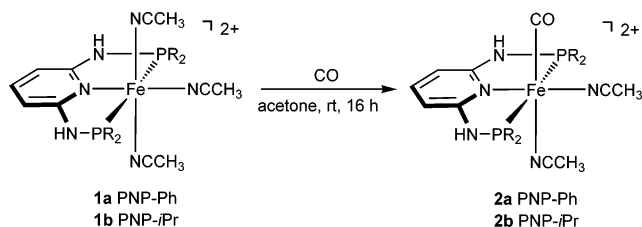
(8) Benito-Garagorri, D.; Becker, E.; Wiedermann, J.; Lackner, W.; Pollak, M.; Mereiter, K.; Kisala, J.; Kirchner, K. *Organometallics* **2006**, *25*, 1900.

(9) (a) Albrecht, M.; van Koten, G. *Angew. Chem.* **2001**, *113*, 3866; *Angew. Chem. Int. Ed.* **2001**, *40*, 3750. (b) van der Boom, M. E.; Milstein, D. *Chem. Rev.* **2003**, *103*, 1759. (c) Rytchinski, B.; Milstein, D. *Angew. Chem.* **1999**, *111*, 918; *Angew. Chem. Int. Ed.* **1999**, *38*, 870. (d) Singleton, J. T. *Tetrahedron* **2003**, *59*, 1837. (e) Vignalok, A.; Milstein, D. *Acc. Chem. Res.* **2001**, *34*, 798. (f) Milstein, D. *Pure Appl. Chem.* **2003**, *75*, 2003. (g) Jensen, C. M. *Chem. Commun.* **1999**, 2443.

Chart 1



Scheme 2



singlet resonance in the $^{31}\text{P}\{^1\text{H}\}$ NMR spectrum at 95.9 and 114.5 ppm, respectively. In the $^{13}\text{C}\{^1\text{H}\}$ NMR spectrum the CO ligand exhibits a low-intensity triplet resonance at 212.4 ($J = 27.0$ Hz) and 215.4 ppm ($J = 25.9$ Hz). The methyl groups of the two inequivalent CH_3CN ligands in **2a** give rise to singlet resonances at 5.1 and 3.4 ppm. In the case of **2b** the resonance of the two MeCN ligands exhibits signals at 3.8 ppm. In the ^1H NMR spectrum the methyl protons of the CH_3CN ligands show signals at 2.58 and 1.58 ppm (**2a**) and 2.53 and 2.40 ppm (**2b**). All other resonances are unremarkable and are not discussed here. In the IR spectrum the CO stretching frequencies for **2a** and **2b** are observed at 2021 and 1995 cm^{-1} , respectively, indicating a weaker π -interaction in the case of **2a** than in **2b** (cf. 2143 cm^{-1} in free CO).

An ORTEP diagram of **2b** is depicted in Figure 1 with selected bond distances and angles reported in the caption. Complex **2b** adopts a distorted octahedral geometry around the metal center with the CO ligand being in *trans* position to an acetonitrile ligand. The PNP ligand is coordinated to the iron center in a typical tridentate meridional mode, with a P–Fe–P angle of 167.6(1)°. The bond lengths around Fe are Fe–P(1) 2.267(1) Å, Fe–P(2) 2.267(1) Å, Fe–N_{py} 1.979(2) Å, Fe–C(18) 1.764(2), Fe–N_{trans} 1.929(2), and Fe–N_{cis} 1.979(2) Å. The Fe–N bond of the nitrile *trans* to the pyridine nitrogen of the PNP ligand is slightly shorter than the one *cis* to the PNP moiety due to the strong *trans* influence of the CO ligand.

A dicarbonyl complex, viz., *cis*-[Fe(PNP–Ph)(CO)₂Br]⁺ (**3**), could be obtained by reacting $\text{Fe}(\text{CO})_4\text{Br}_2$ with 1 equiv of PNP–Ph in the presence of NaBPh_4 in CH_2Cl_2 (Scheme 3). If the reaction was performed with PNP–*i*Pr and PNP–*t*Bu under the same reaction conditions, no clean reaction took place, yielding a mixture of isomers giving rise to several signals in the $^{31}\text{P}\{^1\text{H}\}$ NMR spectrum. Since all attempts to isolate any of these compounds in pure form failed, this reaction was not further investigated. Complex **3** exhibits a singlet resonance in the $^{31}\text{P}\{^1\text{H}\}$ NMR spectrum at 100.5 ppm. In the $^{13}\text{C}\{^1\text{H}\}$ NMR spectrum the two CO ligands exhibit triplet resonances at 209.8 and 206.5 ppm with coupling constants of 20.2 and 23.1 Hz, respectively, clearly indicating that the two CO ligands are *cis* to one another.

Upon treatment of anhydrous FeCl_2 with 1 equiv of PNP–

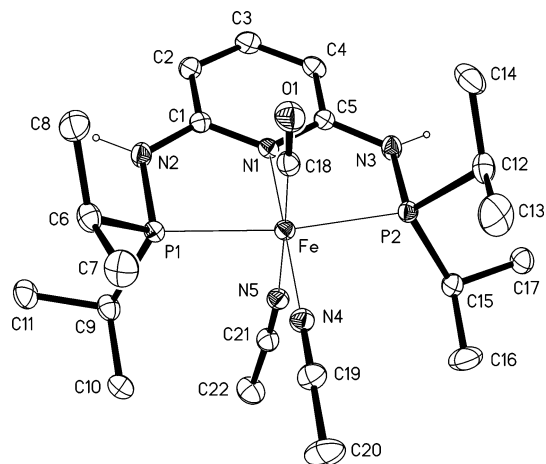
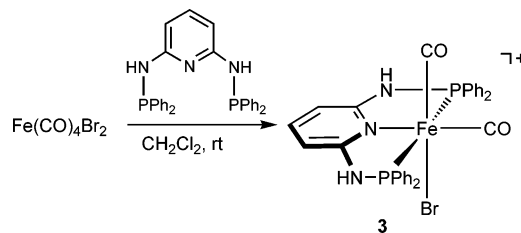
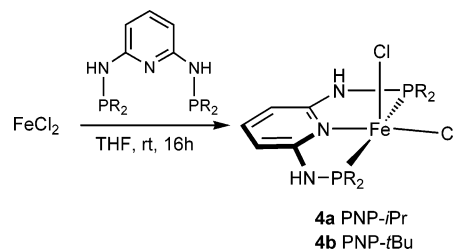


Figure 1. Structural view of *cis*-[Fe(PNP-*i*Pr)(CO)(CH₃CN)₂](BF₄)₂(CH₃)₂CO (**2b**·(CH₃)₂CO) showing 50% thermal ellipsoids (BF₄[−], (CH₃)₂CO, and C-bound H atoms omitted for clarity). Selected bond lengths (Å) and angles (deg): Fe–C(18) 1.7635(16), Fe–N(1) 1.9785(13), Fe–N(4) 1.9286(14), Fe–N(5) 1.9786(14), Fe–P(1) 2.2670(4), Fe–P(2) 2.2674(5), P(1)–N(2) 1.6902(14), P(1)–C(6) 1.8458(16), P(1)–C(9) 1.8428(16), P(2)–N(3) 1.6936(14), P(2)–C(12) 1.8411(17), P(2)–C(15) 1.8404(16), O(1)–C(18) 1.141(2); P(1)–Fe–P(2) 167.59(2).

Scheme 3



Scheme 4



*i*Pr and PNP–*i*Bu in THF at room temperature, the pentacoordinated dichloro complexes [Fe(PNP–*i*Pr)(Cl)₂] (**4a**) and [Fe(PNP–*t*Bu)(Cl)₂] (**4b**), respectively, were obtained in 90 and 84% isolated yields (Scheme 4). These yellow complexes are paramagnetic and display contact-shifted ^1H NMR spectra with relatively narrow line widths at room temperature. In acetone-*d*₆, the ^1H NMR spectrum of **4a** displays all expected ligand resonances, which can be readily assigned on the basis of integration. Diastereotopic isopropyl methyl groups appear at 7.00 (12H) and 13.13 ppm (12H) and the CH protons give rise to a signal at 140.35 ppm (4H), whereas the pyridine hydrogen atoms are centered at 47.49 (2H) and –21.26 (1H). The NH protons exhibit a signal at 75.30 ppm (2H). A concurrent ^1H NMR spectrum is obtained for **4b**.

A structural view of **4b** is depicted in Figure 2 with selected bond distances and angles given in the caption. The coordination geometry of the iron center is distorted square pyramidal with the iron atom lying 0.615(1) Å out of the basal plane (defined by N(1)–P(1)–P(2)–Cl(1)), which show a rms aplanarity of

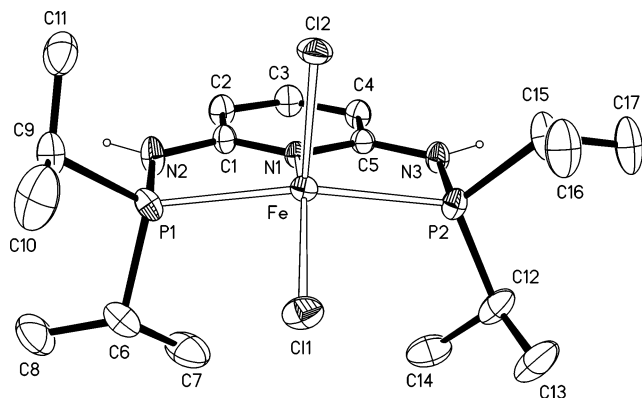


Figure 2. Structural view of $[\text{Fe}(\text{PNP-}i\text{Pr})(\text{Cl})_2](\text{C}_2\text{H}_5)_2\text{O}$ (**4a**) ($\text{C}_2\text{H}_5)_2\text{O}$) showing 30% thermal ellipsoids ($(\text{C}_2\text{H}_5)_2\text{O}$ and C-bound H atoms omitted for clarity). Selected bond lengths (\AA) and angles (deg): Fe–N(1) 2.250(2), Fe–Cl(1) 2.3708(7), Fe–Cl(2) 2.3040(6), Fe–P(1) 2.4631(7), Fe–P(2) 2.4844(7), P(1)–N(2) 1.686(2), P(1)–C(6) 1.877(3), P(1)–C(9) 1.819(3), P(2)–N(3) 1.691(2), P(2)–C(12) 1.832(3), P(2)–C(15) 1.845(3); P(1)–Fe–P(2) 146.56(3), N(1)–Fe–Cl(1) 146.13(6), Cl(2)–Fe–N(1) 106.24(5), Cl(2)–Fe–P(1) 105.19(3), Cl(2)–Fe–P(2) 100.48(3), Cl(2)–Fe–Cl(1) 107.60(3), N(1)–Fe–P(1) 75.95(5), N(1)–Fe–P(2) 76.55(5), Cl(1)–Fe–P(1) 93.75(3), Cl(1)–Fe–P(2) 98.60(3).

0.056 \AA) in the direction of the apical atom Cl(2). This feature is similar to that reported for the five-coordinate complexes $[\text{Fe}(\text{2,6-bis}(\text{diisopropylphosphinomethyl})\text{pyridine})(\text{Cl})_2]$,¹⁰ $[\text{Fe}(\text{2,6-bis}(\text{dimethylaminomethyl})\text{pyridine})(\text{Cl})_2]$,¹¹ $[\text{Fe}(\text{2,6-bis}(\text{2,6-diisopropylphenylaminomethyl})\text{pyridine})(\text{Cl})_2]$,¹² and $[\text{Fe}(\text{2,6-bis}(1-(\text{2,6-diisopropylphenylimino})\text{ethyl})\text{pyridine})(\text{Cl})_2]$.¹³ The bond distance of Fe–P(1) (2.4631(7) \AA) is slightly shorter than that of Fe–P(2) (2.4844(7) \AA). The Fe–Cl(1) (basal) bond, 2.371(1) \AA , is significantly longer than the distance to the apical chlorine (Fe–Cl(2) 2.304(1) \AA).

Catalytic Studies. Some of the complexes of the type $[\text{Fe}(\text{PNP})(\text{CH}_3\text{CN})_3]^{2+}$ reported previously⁹ as well as the new complexes described here were tested as catalyst precursors for the coupling of aromatic aldehydes with EDA. A survey of catalyst activity with *p*-anisaldehyde as model substrate proved that both electronic and steric properties of the ligands are important (Table 1). The most effective catalyst was found to be *cis*- $[\text{Fe}(\text{PNP-}i\text{Pr})(\text{CO})(\text{CH}_3\text{CN})_2]\text{BF}_4$ (**2b**), bearing both strongly electron-donating and bulky *i*Pr substituents in CH_3NO_2 as solvent. No reaction took place in CH_3CN , suggesting that initial dissociation of CH_3CN to form the highly reactive 16e complex $[\text{Fe}(\text{PNP-}i\text{Pr})(\text{CO})(\text{CH}_3\text{CN})]^+$ is important. The use of **2b** leads to very high isolated yields of 3-hydroxyacrylate (84%) with only a trace amount of β -keto ester being formed (<3%). The trisacetonitrile complexes **1a–e** are all less efficient catalysts. Likewise, also complexes *cis*- $[\text{Fe}(\text{PNP-Ph})(\text{CO})_2\text{Br}]\text{BPh}_4$ (**3**) and $[\text{Fe}(\text{PNP-}i\text{Pr})(\text{Cl})_2]$ (**4b**) in both the absence and presence of AgSbF_6 as halide scavenger turned out to be inefficient as catalysts presumably due to decomposition of the complexes. For comparison, with $[\text{FeCp}(\text{CO})_2(\text{THF})]\text{BF}_4$ as catalyst a mixture of 3-hydroxyacrylate (60%) and β -keto ester (20%) was obtained (Table 1, entry 12).

(10) Zhang, J.; Gandelman, M.; Herrman, D.; Leitus, G.; Shimon, L. J. W.; Ben-David, Y.; Milstein, D. *Inorg. Chim. Acta* **2006**, *359*, 1955.

(11) O'Reilly, R. K.; Gibson, V. C.; White, A. J. P.; Williams, D. J. *Polyhedron* **2004**, *23*, 2921.

(12) Britovsek, G. J. P.; Gibson, V. C.; Mastroianni, S.; Oakes, D. C. H.; Redshaw, C.; Solan, G. A.; White, A. J. P.; Williams, D. J. *Eur. J. Inorg. Chem.* **2001**, 431.

(13) Small, B. L.; Brookhart, M.; Bennett, A. M. *J. Am. Chem. Soc.* **1998**, *120*, 4049.

Changing the counterion in **2b** from the weakly coordinating BF_4^- to the noncoordinating anion tetrakis(3,5-ditrifluoromethylphenyl)borate (BArF) (Table 1, entry 7) led to similar yields and reaction rates. Thus, the nature of counterion is apparently not affecting the coupling reaction, as has been frequently observed for Lewis-acid-catalyzed transformations.¹⁴

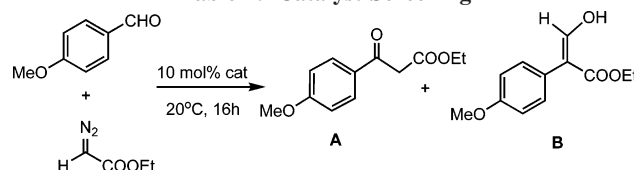
Since this reaction is known to be catalyzed also by simple Lewis acids such as $\text{HBF}_4 \cdot \text{Et}_2\text{O}$,⁴ the acidic NH hydrogen atoms of complexes **1–4** may release H^+ , being thus an additional or even the sole source of the catalytically active species. In order to rule out this possibility, complex **1d** ($[\text{Fe}(\text{PNP-Ph}^{\text{Hex}})(\text{CH}_3\text{CN})_3](\text{BF}_4)_2$), which lacks acidic NH hydrogen atoms, was also utilized as a catalyst showing even higher activity than **1a**, which features acidic NH protons at the PNP ligand but bears also phenyl substituents at the phosphorus atoms.

The effect of catalyst loading and reaction rate was then determined using the same reaction conditions (Figure 3). The reaction proceeds well with 10 mol % of catalyst **2b**, showing after 24 h a conversion of 95 and 83% for *p*-fluorobenzaldehyde and *p*-anisaldehyde, respectively, with TONs in the range from 2.2 to 8.9. However, the conversion decreases to 60 and 50% after the catalyst loading is decreased to 1 mol % (TONs: 23 to 60), which may be attributed to catalyst decomposition.

To investigate the scope and limitations of the iron PNP system, complex **2b** was used as catalyst. A survey of the reactivity of EDA with various aromatic aldehydes under catalytic conditions is provided in Table 2. Operationally, both EDA and aldehyde were added together in a 1:1 ratio in CH_3NO_2 as the solvent and the solution was stirred for 16 h at room temperature. Although the catalytic reactions were routinely performed under an inert Ar atmosphere, admission of air did not affect the yields. In all cases 3-hydroxyacrylates, as judged from the ^1H NMR spectra of the crude reaction mixture, were formed selectively. The formation of β -keto esters is <3%, while the formation of epoxides was not observed in any of these reactions. This is in contrast to the catalytic reactions of $[\text{FeCp}(\text{CO})_2(\text{THF})]\text{BF}_4$ with aromatic aldehydes and EDA, where mixtures of 3-hydroxyacrylates and β -keto esters were observed. For instance, the reaction of benzaldehyde and EDA at 25 $^\circ\text{C}$ with $[\text{FeCp}(\text{CO})_2(\text{THF})]\text{BF}_4$ as catalysts (10 mol %) affords a mixture of 3-hydroxy-2-phenylacrylic acid ethyl ester and 3-oxo-3-phenylpropionic acid ethyl ester in 58 and 25% yields.^{4a} The same reaction performed with **2b** yields almost exclusively 3-hydroxy-2-phenylacrylic acid ethyl ester in 91% yield (Table 2, entry 7). With the exception of *p*-dimethylaminobenzaldehyde (entry 5), the yields of 3-hydroxyacrylates are in the range 74 to 91%. The catalytic effect of the iron complexes was confirmed by running the standard reaction, i.e., *p*-anisaldehyde and EDA, without catalyst. No product was formed and only starting materials were isolated from the reaction mixture.

A tentative mechanistic proposal for the coupling of aromatic aldehydes with EDA catalyzed by *cis*- $[\text{Fe}(\text{PNP-}i\text{Pr})(\text{CO})(\text{CH}_3\text{CN})_2]^{2+}$ is presented in Scheme 5, which is similar to the one suggested by Hossain et al.^{4a} Since CO exhibits a much stronger *trans* effect (and *trans* influence) than pyridine, the CH_3CN ligand *trans* to CO is more labile than the one *trans* to the pyridine moiety of the PNP ligand. This fact may also account for the higher reactivity of **2b** as compared to **1b**. Accordingly, substitution of this ligand by an aldehyde molecule (which is present in large excess under catalytic conditions) may afford $[\text{Fe}(\text{PNP-}i\text{Pr})(\text{CO})(\text{CH}_3\text{CN})(\kappa^1(\text{O})\text{-aldehyde})]^{2+}$ (**A**). Nucleophilic attack of EDA to the coordinated aldehyde via a $\text{S}_{\text{N}}2$ -

(14) Kündig, E. P.; Saudan, C. M.; Bernardinelli, G. *Angew. Chem., Int. Ed.* **1999**, *38*, 1219.

Table 1. Catalyst Screening^a

| entry | catalyst | yield (%) A | yield (%) B |
|-------|--|-------------|-------------|
| 1 | [Fe(PNP-Ph)(CH ₃ CN) ₃](BF ₄) ₂ (1a) | <3 | 21 |
| 2 | [Fe(PNP- <i>i</i> Pr)(CH ₃ CN) ₃](BF ₄) ₂ (1b) | <3 | 66 |
| 3 | [Fe(PNP-BIPOL)(CH ₃ CN) ₃](BF ₄) ₂ (1c) | <3 | 53 |
| 4 | [Fe(PNP-Ph ^{Hex})(CH ₃ CN) ₃](BF ₄) ₂ (1d) | <3 | 49 |
| 5 | [Fe(PNP ^T -Ph)(CH ₃ CN) ₃](BF ₄) ₂ (1e) | <3 | 44 |
| 6 | <i>cis</i> -[Fe(PNP- <i>i</i> Pr)(CO)(CH ₃ CN) ₂](BF ₄) ₂ (2b) | <3 | 84 |
| 7 | <i>cis</i> -[Fe(PNP- <i>i</i> Pr)(CO)(CH ₃ CN) ₂](BArF) ₂ (2b) ^b | <3 | 80 |
| 8 | <i>cis</i> -[Fe(PNP-Ph)(CO) ₂ (Br)]BPh ₄ (3) | 0 | 0 |
| 9 | <i>cis</i> -[Fe(PNP-Ph)(CO) ₂ (Br)]BPh ₄ (3) + AgSbF ₆ (1 equiv) | <3 | 13 |
| 10 | [Fe(PNP- <i>i</i> Pr)(Cl) ₂] (4) + AgSbF ₆ (1 equiv) | <3 | 26 |
| 11 | [Fe(PNP- <i>i</i> Pr)(Cl) ₂] (4) + AgSbF ₆ (2 equiv) | <3 | 37 |
| 12 | [FeCp(CO) ₂ (THF)]BF ₄ ^c | 20 | 60 |

^a Reaction conditions: 1 equiv of aldehyde, 1 equiv of EDA, rt, CH₃NO₂ as the solvent, reaction time 16 h; yields represent isolated yields (average of at least three experiments). ^bBArF = tetrakis(3,5-ditrifluoromethylphenyl)borate. ^c1.2 equiv of aldehyde, 1 equiv of EDA, 0 °C, CH₂Cl₂ as the solvent, overall reaction time 16 h; isolated yields (ref 4a).

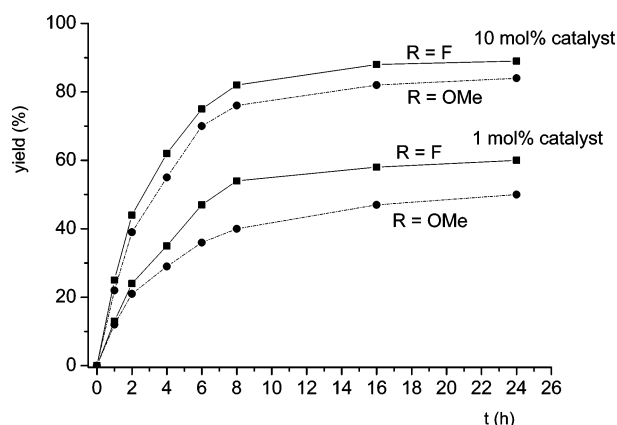


Figure 3. Plot of yield versus time for the formation of 3-hydroxyacrylates from *p*-fluorobenzaldehyde and *p*-anisaldehyde with EDA utilizing 10 and 1 mol %, respectively, of *cis*-[Fe(PNP-*i*Pr)(CO)(CH₃CN)₂](BF₄)₂ (**2b**) as catalyst.

type mechanism yields, via transition state **B**, intermediate **C**. In the course of this step N₂ is liberated. Preferential migration of the aryl substituent over hydride migration leads eventually to intermediate **D**, featuring an κ^1 (O)-coordinated aldehyde ester ligand. After liberation of the ester aldehyde by incoming aldehyde substrates, this molecule rapidly tautomerizes to yield the thermodynamically more stable respective 3-hydroxyacrylates.

In principle, an alternative pathway could proceed via formation of the epoxide ethyl-3-arylglycidate from complex **C** and subsequent rearrangement to the corresponding enol ester, since it is known that transition metal complexes are able to convert epoxides to ketones and aldehydes.¹⁵ This mechanism was dismissed however since formation of 3-hydroxy-2-phenylacrylic acid ethyl ester from ethyl-3-phenylglycidate in the presence **2b** under the same reaction conditions was not observed.

A mechanism where in the initial step both aldehyde and EDA are coordinated, as proposed by Kanemasa et al., seems to be

less likely but cannot be completely ruled out at this stage. Likewise, the intermediacy of carbenes may have been taken into account. In this context it has to be mentioned that **2b** does not react with EDA in the absence of aldehydes.

In summary, a general and efficient protocol for the coupling of aromatic aldehydes with EDA has been developed. The catalyst is part of a new generation of air-stable, well-defined iron PNP pincer-type systems. Investigations into the use of these compounds as catalysts in the coupling of EDA with ketones, lactones, and lactams are ongoing. A detailed mechanistic investigation based on DFT/B3LYP calculations is currently also being pursued and will be reported in due course.

Experimental Section

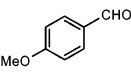
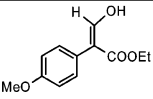
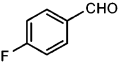
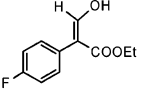
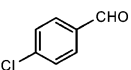
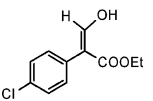
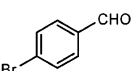
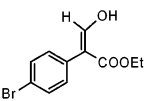
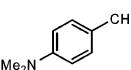
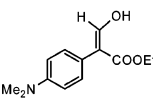
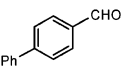
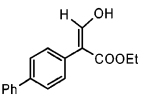
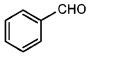
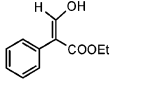
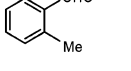
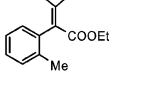
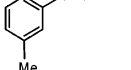
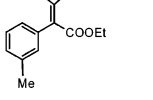
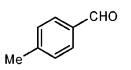
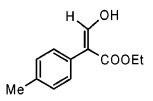
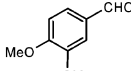
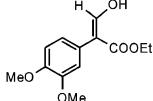
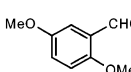
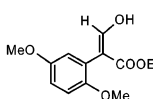
General Procedures. All manipulations were performed under an inert atmosphere of argon by using Schlenk techniques. The solvents were purified according to standard procedures.¹⁶ *N,N'*-Bis(diphenylphosphino)-2,6-diaminopyridine (PNP-Ph), *N,N'*-bis(diisopropylphosphino)-2,6-diaminopyridine (PNP-*i*Pr), *N,N'*-bis(di-*tert*-butylphosphino)-2,6-diaminopyridine (PNP-*t*Bu), [Fe(PNP-Ph)(CH₃CN)₃](BF₄)₂ (**1a**), [Fe(PNP-*i*Pr)(CH₃CN)₃](BF₄)₂ (**1b**), [Fe(PNP-BIPOL)(CH₃CN)₃](BF₄)₂ (**1c**), [Fe(PNP-Ph^{Hex})(CH₃CN)₃](BF₄)₂ (**1d**), and [Fe(PNP^T-Ph)(CH₃CN)₃](BF₄)₂ (**1e**) were prepared according to the literature.⁹ The deuterated solvents were purchased from Aldrich and dried over 4 Å molecular sieves. ¹H, ¹³C{¹H}, and ³¹P{¹H} NMR spectra were recorded on a Bruker AVANCE-250 spectrometer and were referenced to SiMe₄ and H₃PO₄ (85%), respectively. ¹H and ¹³C{¹H} NMR signal assignments were confirmed by ¹H-COSY, 135-DEPT, and HMQC(¹H-¹³C) experiments.

cis-[Fe(PNP-Ph)(CO)(CH₃CN)₂](BF₄)₂ (**2a**). Carbon monoxide was bubbled into a solution of **1a** (0.5 g, 0.6 mmol) in acetone (30 mL) for 15 min, whereupon the color of the solution turned from orange to yellow, and the mixture was stirred overnight at room temperature under CO atmosphere. After removal of the solvent under reduced pressure, the remaining yellow solid was washed twice with Et₂O (20 mL) and dried under vacuum. Yield: 0.4 g (88%). Anal. Calcd for C₃₄H₃₁B₂F₈FeN₅OP₂: C, 49.98; H, 3.82; N, 8.57. Found: C, 49.93; H, 3.71; N, 8.40. ¹H NMR (δ , acetone-*d*₆, 20 °C): 9.21 (s, 2H, NH), 7.99–7.84 (m, 7H, Ph and py⁴),

(15) (a) Maruoka, K.; Nagahara, S.; Ooi, T.; Yamamoto, H. *Tetrahedron Lett.* **1989**, 30, 5607. (b) Miyashita, A.; Shimada, T.; Sugawara, A.; Nohira, H. *Chem. Lett.* **1986**, 1323.

(16) Perrin, D. D.; Armarego, W. L. F. *Purification of Laboratory Chemicals*, 3rd ed.; Pergamon: New York, 1988.

Table 2. Yields of 3-Hydroxyacrylates from the Reactions of Aromatic Aldehydes with EDA Catalyzed by *cis*-[Fe(PNP-*i*Pr)(CO)(CH₃CN)₂](BF₄)₂ (**2**)^{a,b}

| entry | aldehyde | 3-hydroxyacrylate | % |
|-------|---|---|----|
| 1 |  |  | 84 |
| 2 |  |  | 88 |
| 3 |  |  | 86 |
| 4 |  |  | 86 |
| 5 |  |  | 58 |
| 6 |  |  | 83 |
| 7 |  |  | 91 |
| 8 |  |  | 78 |
| 9 |  |  | 89 |
| 10 |  |  | 84 |
| 11 |  |  | 74 |
| 12 |  |  | 80 |

^a Reaction conditions: 1 equiv of aldehyde, 1 equiv of EDA, 10 mol % catalyst, CH₃NO₂ as the solvent, rt, reaction time 16 h. Yields represent isolated yields (average of at least three experiments). ^bThe yield of β -keto ester is <3%.

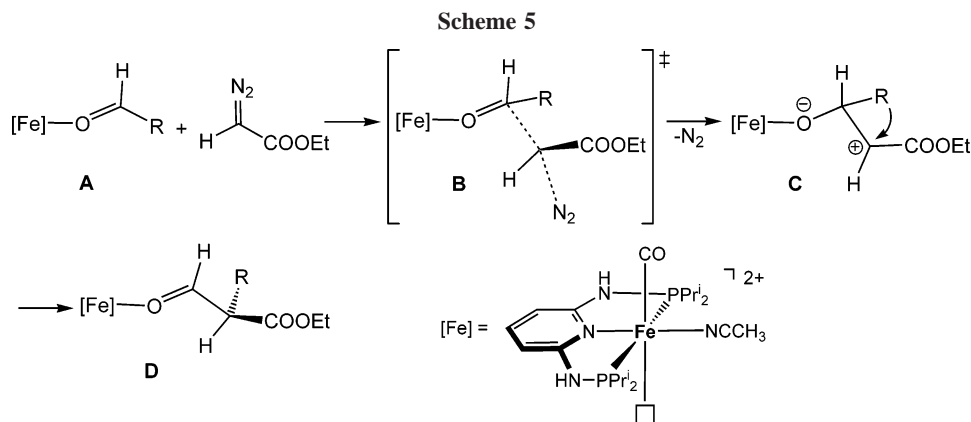
7.56–7.40 (m, 14H, Ph), 6.70 (d, $J = 7.4$ Hz, 2H, py^{3,5}), 2.58 (s, 3H, CH₃CN), 1.58 (s, 3H, CH₃CN). ¹³C{¹H} NMR (δ , acetone-*d*₆, 20 °C): 212.4 (t, $J = 27.0$ Hz, CO), 162.6 (t, $J = 8.3$ Hz, py^{2,6}), 143.6 (py⁴), 140.2 (Ph¹), 133.4 (CH₃CN), 133.1 (CH₃CN), 132.1–131.7 (m, Ph), 130.7–130.4 (m, Ph), 103.2 (t, $J = 4.1$ Hz, py^{3,5}), 5.1 (CH₃CN), 3.4 (CH₃CN). ³¹P{¹H} NMR (δ , acetone-*d*₆, 20 °C): 95.9. IR (KBr, cm⁻¹): 2021 ($\nu_{C=O}$).

cis-[Fe(PNP-*i*Pr)(CO)(CH₃CN)₂](BF₄)₂ (**2b**). This complex has been prepared analogously to **2a** with **1b** (1.5 g, 2.2 mmol) and CO as the starting materials. Yield: 1.4 g (93%). Anal. Calcd for C₂₂H₃₉B₂F₈FeN₅O₂: C, 38.80; H, 5.77; N, 10.28. Found: C, 38.90; H, 5.71; N, 10.21. ¹H NMR (δ , acetone-*d*₆, 20 °C): 7.39 (s, 1H, py⁴), 6.90 (s, 2H, NH), 6.34 (s, 2H, py^{3,5}), 3.17 (s, 4H, CH(CH₃)₂), 2.53 (s, 3H, CH₃CN), 2.40 (s, 3H, CH₃CN), 1.56–1.50 (m, 24H, CH(CH₃)₂). ¹³C{¹H} NMR (δ , acetone-*d*₆, 20 °C): 215.4 (t, $J = 25.9$ Hz, CO), 162.1 (t, $J = 6.6$ Hz, py^{2,6}), 141.8 (t, $J = 38.8$ Hz, py⁴), 139.8 (CH₃CN), 100.59 (t, $J = 3.5$ Hz, py^{3,5}), 27.87 (t, $J = 13.0$ Hz, CH(CH₃)₂), 17.7 (d, $J = 29.7$ Hz, CH(CH₃)₂), 17.0 (d, $J = 29.1$ Hz, CH(CH₃)₂), 3.8 (d, $J = 10.1$ Hz, CH₃CN). ³¹P{¹H} NMR (δ , acetone-*d*₆, 20 °C): 114.7. IR (KBr, cm⁻¹): 1995 ($\nu_{C=O}$).

cis-[Fe(PNP-*i*Pr)(CO)(CH₃CN)₂](BArF)₂ (**2b'**). To a stirred suspension of **2b** (100 mg, 0.14 mmol) in CH₂Cl₂ (10 mL) was added sodium tetrakis(3,5-difluoromethylphenyl)borate (260 mg, 0.29 mmol), and the mixture was stirred for 2 h. During that time the solution turned yellow and a white solid (NaBF₄) was formed. Solid materials were removed by filtration. The solvent was then removed under reduced pressure, affording a yellow solid, which was dried under vacuum. Yield: 275 mg (88%). Anal. Calcd for C₈₆H₆₃B₂F₄₈FeN₅O₂: C, 46.24; H, 2.84; N, 3.14. Found: C, 46.19; H, 2.90; N, 3.25. ¹H NMR (δ , CD₂Cl₂, 20 °C): 7.72 (bs, 16 H, BArF), 7.57 (bs, 8H, BArF), 7.33 (t, $J = 8.4$ Hz, 1H, py⁴), 6.30 (d, $J = 8.4$ Hz, 2H, py^{3,5}), 5.68 (s, 2H, NH), 3.08 (bs, 2H, CH(CH₃)₂), 2.90 (bs, 2H, CH(CH₃)₂), 2.46 (s, 3H, CH₃CN), 2.30 (s, 3H, CH₃CN), 1.55–1.24 (m, 24H, CH(CH₃)₂). ¹³C{¹H} NMR (δ , CD₂Cl₂, 20 °C): 219.9 (CO), 161.7 (q, $J = 49.7$ Hz, BArF), 161.1 (py^{2,6}), 143.1 (py⁴), 134.7 (BArF), 133.6 (CH₃CN), 128.8 (q, $J = 32.2$ Hz, BArF), 124.5 (q, $J = 270.7$ Hz, BArF), 117.5 (BArF), 102.1 (py^{3,5}), 29.6 (t, $J = 10.4$ Hz, CH(CH₃)₂), 28.9 (t, $J = 12.3$ Hz, CH(CH₃)₂), 17.6 (t, $J = 5.7$ Hz, CH(CH₃)₂), 4.65 (CH₃CN), 4.47 (CH₃CN). ³¹P{¹H} NMR (δ , CD₂Cl₂, 20 °C): 114.5.

cis-[Fe(PNP-Ph)(CO)₂(Br)]BPh₄ (**3**). To a solution of Fe(CO)₄Br₂ (250 mg, 0.76 mmol) and NaBPh₄ (261 mg, 0.76 mmol) in CH₂Cl₂ was added PNP-Ph (364 mg, 0.76 mmol), resulting in significant gas evolution. The solution was stirred until no further gas evolution was observed. Insoluble materials (NaBr) were then removed by filtration. After removal of the solvent under reduced pressure, the remaining orange solid was washed twice with Et₂O (20 mL) and dried under vacuum. Yield: 417 mg (82%). Anal. Calcd for C₅₅H₄₅BBrFeN₃O₂P₂: C, 66.83; H, 4.59; N, 4.25. Found: C, 66.94; H, 4.66; N, 4.35. ¹H NMR (δ , CD₂Cl₂, 20 °C): 7.90 (s, 2H, NH), 7.79–7.77 (m, 3H, Ph), 7.66–7.64 (m, 4H, Ph), 7.48–7.45 (m, 20H, Ph and py⁴), 7.02–7.00 (m, 10H, Ph), 6.85–6.82 (m, 4H, Ph), 6.59–6.56 (d, $J = 7.9$ Hz, py^{3,5}). ¹³C{¹H} NMR (δ , CD₂Cl₂, 20 °C): 209.8 (t, $J = 20.2$ Hz, CO), 206.5 (t, $J = 23.1$ Hz, CO), 164.0 (q, $J = 49.32$ Hz, BPh₄), 159.3 (t, $J = 8.67$ Hz, py^{2,6}), 142.4 (py⁴), 136.0 (BPh₄), 132.2 (PPh₂), 132.0 (PPh₁), 130.0 (PPh₄), 129.9 (PPh^{3,5}), 125.8 (BPh₄), 122.0 (BPh₄), 102.7 (py^{3,5}). ³¹P{¹H} NMR (δ , CD₂Cl₂, 20 °C): 100.5.

[Fe(PNP-*i*Pr)(Cl)₂] (**4a**). FeCl₂ (180 mg, 1.46 mmol) was added to a solution of PNP-*i*Pr (500 mg, 1.46 mmol) in THF, and the reaction mixture was stirred overnight at room temperature. The yellow solution was then filtered, and the solvent was evaporated under reduced pressure. The remaining yellow solid was washed twice with Et₂O (10 mL) and dried under vacuum. Yield: 615 mg (90%). Anal. Calcd for C₁₇H₃₃Cl₂FeN₃P₂: C, 43.61; H, 7.10; N, 8.98. Found: C, 43.70; H, 7.16; N, 8.87. ¹H NMR (δ , acetone-*d*₆,



20 °C, all peaks appear as broad singlets): 140.35 ($\text{CH}(\text{CH}_3)_2$), 75.30 (NH), 47.49 ($\text{py}^{3,5}$), 13.13 ($\text{CH}(\text{CH}_3)_2$), 7.00 ($\text{CH}(\text{CH}_3)_2$), -21.26 (py^4). The identity of the NH protons was determined by adding 0.2 mL of D_2O to the NMR tube, whereupon the signal at 75.30 ppm disappeared.

[Fe(PNP-*t*Bu)(Cl)₂] (4b). This complex has been prepared analogously to **4a** with FeCl_2 (100 mg, 0.78 mmol) and PNP-*t*Bu (314 mg, 0.78 mmol) as the starting materials. Yield: 343 mg (84%). Anal. Calcd for $\text{C}_{21}\text{H}_{41}\text{Cl}_2\text{FeN}_3\text{P}_2$: C, 48.11; H, 7.88; N, 8.01. Found: C, 48.21; H, 7.79; N, 8.11. ^1H NMR (δ , acetone- d_6 , 20 °C, all peaks appear as broad singlets): 64.68 (NH), 51.57 ($\text{py}^{3,5}$), 17.46 (CH_3), -20.18 (py^4).

General Procedure for the Iron(II)-Catalyzed Synthesis of 3-Hydroxyacrylates. Aldehyde (1 equiv) and ethyldiazoacetate (1 equiv) were added to a solution of the catalyst (10 mol %) in CH_3NO_2 (5 mL), and the mixture was stirred at room temperature for 16 h. The mixture was then filtered through a plug of silica to remove the catalyst, and the product was purified by flash chromatography (silica, CH_2Cl_2).

X-ray Structure Determination. X-ray data for *cis*-[Fe(PNP-*i*Pr)(CO)(CH_3CN)₂](BF_4)₂·(CH_3)₂CO (**2**·(CH_3)₂CO) and [Fe(PNP-*i*Pr)(Cl)₂·(C_2H_5)₂O (**4a**·(C_2H_5)₂O) were collected on a Bruker Smart APEX CCD area detector diffractometer at $T = 100$ K using graphite-monochromated Mo $\text{K}\alpha$ radiation ($\lambda = 0.71073$ Å) and 0.3° ω -scan frames covering complete spheres of the reciprocal space with $\theta_{\text{max}} = 30^\circ$. After data integration with the program SAINT corrections for absorption, $\lambda/2$ effects, and crystal decay were applied with SADABS.¹⁷ The structures were solved by direct methods using the program SHELXS97.¹⁸ Structure refinement on

F^2 was carried out with the program SHELXL97.¹⁷ All non-hydrogen atoms were refined anisotropically. Hydrogen atoms were inserted in idealized positions and were refined riding with the atoms to which they were bonded.

Crystal data: **2b**·(CH_3)₂CO: $\text{C}_{25}\text{H}_{45}\text{B}_2\text{F}_8\text{FeN}_5\text{O}_2\text{P}_2$, $M_r = 739.07$, monoclinic, space group $P2_1/c$ (no. 14), $T = 100$ K, $a = 10.8683(9)$ Å, $b = 10.4976(8)$ Å, $c = 29.963(2)$ Å, $\beta = 99.796(2)^\circ$, $V = 3368.7(4)$ Å³, $Z = 4$, $\mu = 0.619$ mm⁻¹. Of 44 797 reflections collected, 9753 were independent; final R indices: $R_1 = 0.047$ (all data), $wR_1 = 0.098$ (all data). Crystal data of **4a**·(C_2H_5)₂O: $\text{C}_{21}\text{H}_{43}\text{Cl}_2\text{FeN}_3\text{OP}_2$, $M_r = 542.27$, orthorhombic, space group $P2_12_12_1$ (no. 19), $T = 100$ K, $a = 9.6583(5)$ Å, $b = 14.5653(7)$ Å, $c = 20.2207(10)$ Å, $V = 2844.6(2)$ Å³, $Z = 4$, $\mu = 0.847$ mm⁻¹. Of 32 002 reflections collected, 8261 were independent; final R indices: $R_1 = 0.043$ (all data), $wR_1 = 0.113$ (all data). Further details (atomic coordinates, displacement parameters, etc.) and geometric data are given in the Supporting Information in CIF format.

Acknowledgment. Financial support by the “Fonds zur Förderung der Wissenschaftlichen Forschung” is gratefully acknowledged (Project No. P16600-N11). D.B.-G. thanks the Basque Government (Eusko Jaurilaritza/Gobierno Vasco) for a doctoral fellowship.

Supporting Information Available: Spectroscopic data of all organic compounds. Complete crystallographic data and technical details in CIF format for **2b**·(CH_3)₂CO and **4b**·(C_2H_5)₂O. This material is available free of charge via the Internet at <http://pubs.acs.org>.

OM0608020

(17) Bruker programs: *SMART*, version 5.629; *SAINT*, version 6.45; *SADABS*, version 2.10; *SHELXTL*, version 6.14; Bruker AXS Inc.: Madison, WI, 2003.

(18) Sheldrick, G. M. *SHELX97*, Program System for Crystal Structure Determination; University of Göttingen: Göttingen, Germany, 1997.